RSC Advances

ROYAL SOCIETY OF CHEMISTRY

www.rsc.org/advances

Journal Name

ARTICLE

Enhanced electrochemical performance of lamellar structured Co-Ni(OH)$_2$ /reduced Graphene Oxide (rGO) via hydrothermal synthesis

Received 00th January 20xx,
Accepted 00th January 20xx

DOI: 10.1039/x0xx00000x

www.rsc.org/

Sintayehu Nibret Tiruneh,‡[a] Bong Kyun Kang,‡[a] Quang Tran Ngoc[a] and DaeHo Yoon [*ab]

Lamellar Co-Ni(OH)$_2$/rGO structures were prepared by co-precipitation followed by hydrothermal synthesis. Lamellar and crystalline Co-Ni(OH)$_2$/rGO delivered better specific capacitance (Cs) and rate capability than low-crystallinity composites due to improved ionic and electronic conductivity. A high value of the Cs was achieved with Co-Ni(OH)$_2$/rGO prepared at 150 °C for 12 h with a graphite oxide (GO)-to-metal precursor ratio of 1:5. This condition gave a Cs of 617 F g^{-1} at 2 mV s^{-1} and 811 F g^{-1} at 0.5 A g^{-1} with the highest capacitance retention of 90 % at 2 A g^{-1} and good cycling stability (~77 % at 70 mV s^{-1}) at 5000 cycles. Furthermore, high mass loading, ~4.5-5.5 mg cm^{-2}, was used in the fabrication of the electrodes, which is higher than that of most previous reports.

Introduction

Supercapacitors (SCs) are advanced versions of the prosaic capacitors which have been in use since the early days of radio. The conventional capacitors have quite modest energy-holding capacity and short lives. SCs offer an emerging advanced energy storage solution that bridges the gap between conventional capacitors and rechargeable batteries.[1] This technology will develop based mainly on its adoption in transportation applications such as hybrid buses, in consumer electronics, and with wind turbines - all of which now play more significant roles in our lives.[2]

Pseudocapacitive materials including transition metal oxides, metal hydroxides (MHs), nitride sulphides, and conducting polymers can exhibit multiple oxidation states in which they are capable of rich redox reactions. Among these, nickel hydroxide has received increased attention for application in SCs, especially due to its electrochemical properties and potential applications in rechargeable nickel-based alkaline batteries.[3] Hence, it has been used as an electrode material for battery technologies since the first half of the 20th century. Nonetheless, Ni(OH)$_2$ has low electrical conductivity (10^{-5} to 10^{-9} S cm^{-1}) which inhibits its performance in SC applications.[4,5] Several methods can be employed to improve the electrochemical performance of Ni(OH)$_2$, which is compromised by its poor electrical conductivity. These methods include coupling Ni(OH)$_2$ with conductive materials such as graphene, doping or substitution for the Ni atom with other elements, synthesizing new structures, and enhancing the crystallinity of Ni(OH)$_2$.[6-8] Wang et al. reported Ni(OH)$_2$ nanoplates grown on highly conducting graphene using the two step, hydrolysis-solvothermal method.[9] The nanoplates/graphene composite exhibited high specific capacitance (Cs) ~ 1335 F g^{-1} and good stability but with a very small mass loading of 1 mg cm^{-2}. P. Huang et al. used a solvothermal method to synthesize three-dimensional sandwich-like cobalt nickel aluminium layered double hydroxides with different amounts of rGO and obtained a high Cs ~ 1866 F g^{-1} at 1 A g^{-1} with a small mass loading of 2 mg cm^{-2}.[8] The solvothermal method used in both studies is expensive compared to hydrothermal synthesis due to the cost of the solvents used, which were respectively N,N-dimethylformamide and anhydrous methanol. Moreover, very small mass loadings were utilized in the electrochemical measurements - far beyond the current mass loading of electrode materials in commercial supercapacitors of ~10 mg cm^{-2}.[10]

Yingwen Cheng et al. prepared self-supporting electrodes from a Co-Ni(OH)$_2$/graphene binary composite, obtaining very high Cs ~ 2360 F g^{-1}, by integrating the composite with carbon nanotubes (CNTs) during electrode fabrication.[4] In spite of the high capacitance, the samples used as an electrode were of low crystallinity. Additionally, when CNTs were not utilized in the electrode fabrication step, the composite delivered only 1000 F g^{-1}. It is known that the movement of ions and electrons between the inner and outer boundaries of electrode materials is vital for high-performance SCs.[11-13]

[a] School of Advanced Materials Science and Engineering, Sungkyunkwan University, South Korea.
[b] SKKU Advanced Institute of Nanotechnology (SAINT), Sungkyunkwan University, South Korea.

†Electronic Supplementary Information (ESI) available:. See DOI: 10.1039/x0xx00000x

‡ S.NibretTiruneh and B. K. Kang contributed equally to this work.

Graphene has attracted gigantic attention all over the world owing to its large surface area (2600 $m^2 g^{-1}$), high conductivity (10^3-10^4 S m^{-1}), and excellent mechanical, electronic, and thermal properties.[14,15] Thus, incorporation of graphene into MHs will significantly improve their conductivity. Consequently, for enhancement of the electrochemical performance of SCs it is essential to find a material with a structure that strongly supports ion transfer and facilitates electron conduction. In addition, low-crystallinity materials usually suffer from low electronic conductivity when applied as electrode materials. This can be due to the presence of very open microstructures in an amorphous or low-crystallinity state. Conversely, studies showed that by improving the crystallinity of the electrode material it is possible to enhance the discharging capability.[16] Accordingly, it is crucial to consider product morphology, crystallinity, mass loading, and ease of synthesis (solvothermal or hydrothermal) when developing electrode materials for SCs - in order to acquire the desired electrochemical properties such as high capacity and high discharging capability, as well as to fulfil the commercial requirement of higher mass loading. Herein, we report the synthesis of unique lamellar Co-$Ni(OH)_2$/rGO structures through co-precipitation followed by hydrothermal synthesis. The thus-obtained lamellar structures delivered a high Cs at a higher mass loading due to their unique structure, which is comprised of coatings of MHs on the tops and bottoms of rGO layers, amounting to the rGO being sandwiched by the MHs. Moreover, good electrochemical stability, ~77 % at 70 mV s^{-1}, at 5000 cycles can be attributed to the unique lamellar structure which has highly coupled MHs with conductive rGO sheets. In addition, the effect of crystallinity on the specific capacitance is reported. High mass loading, ~4.5-5.5 mg cm^{-2}, was realized in the fabrication of the electrodes, which is higher than that in most previous reports.[8,17-19]

Experimental

Synthesis of GO and Graphene Oxide dispersion

GO was first prepared by using the modified Hummer's method from natural graphite flakes.[20] The GO was then dispersed in deionized (DI) water at different concentrations and sonicated for 3 h at room temperature (RT) to give graphene oxide dispersion.

Preparation of Co-$Ni(OH)_2$/rGO at RT

Equal mass ratios of $Co(NO_3)_2 \cdot 6H_2O$ and $Ni(NO_3)_2 \cdot 6H_2O$ were added in a beaker containing 28 mL of graphene oxide dispersion and stirred for 15 minutes; this allowed adsorption of the metal ions on the surface of the graphene oxide sheets. Ammonium hydroxide (NH_4OH) was used as a precipitant and added dropwise until the pH of the solution reached 9 with continuous stirring. The color of the solution was changed from black to dark green when pH reached 9, which can be assumed as the completion of precipitation. $N_2H_4 \cdot H_2O$ (1 µl mg^{-1} GO) was added to reduce the prepared MHs/graphene oxide solution. The solution was then washed with DI water several times and filtered through 1 µm polytetrafluoroethylene (PTFE) filter membrane and freeze dried for 24 h.

Preparation of Co-$Ni(OH)_2$/rGO at different hydrothermal synthesis temperatures

All subsequent steps were the same as those for the sample obtained at RT, except that before the washing step, the obtained MHs/graphene oxide solution was transferred to a 60 ml Teflon lined stainless steel autoclave and maintained at different hydrothermal synthesis temperatures for 10 h.

Sample Characterization

The surface morphology of the as prepared samples were characterized using a field emission scanning electron microscope (FESEM, JEOL 7500F). A transmission electron microscope (TEM), High Resolution TEM (HRTEM, 200 kV), and selected area electron diffraction (SAED) were also employed to analyze the microstructures of the prepared samples. To study the composition of the obtained products, energy dispersive x-ray spectroscopy (EDS) mapping and x-ray photoelectron spectroscopy (XPS) were applied. Furthermore, the structure, crystallinity, and phases involved in the Co-$Ni(OH)_2$/rGO composites were assessed using X-ray diffraction (PDR-XRD, Bruker D8 FOCUS) with Cukα radiation.

Electrochemical measurements were carried out in a three-electrode system. The measurements were performed at a VMP3 electrochemical workstation (instruments from Bio-logic Science, France). Co-$Ni(OH)_2$/rGO powders were mixed with carbon black as the conducting agent and PTFE as a binder at an 8:1:1 ratio using the solvent 2-propanol to form a slurry. The mixed slurry was then pasted on nickel foam which was initially treated with HCl to remove surface oxides. The mass loading on the nickel foam was in the range of 4.5-5.5 mg cm^{-2}. Cyclic Voltammetry (CV) (with a window potential of 0 - 0.5 V) and Galvanostatic Charge Discharge (GCD) tests (0 - 0.38 V) were carried out using loaded samples on Ni foam as a working electrode, Ag/AgCl as a reference electrode, and Pt wire as a counter electrode in a 2M KOH aqueous solution as the electrolyte at room temperature.

Results and discussion

Co-$Ni(OH)_2$/rGO composites were prepared by co-precipitation followed by hydrothermal synthesis, as schematically depicted in Fig. 1a. First, the graphene oxide dispersion was prepared from GO through sonication. Then metal precursors $Co(NO_3)_2 \cdot 6H_2O$ and $Ni(NO_3)_2 \cdot 6H_2O$ were dissolved in the dispersion. The metal salts were adsorbed on the graphene oxide surface due to the presence of various functional groups (epoxy, carbonyl, and hydroxyl) which act as anchoring sites.[21] NH_4OH was added dropwise, which allowed the formation of metal ammonia complexes leading to precipitation of MHs at pH = 9.[22] Consequently, the mixture was treated with $N_2H_4 \cdot H_2O$ to reduce the GO surface to make it more conductive.[23] In the sample obtained from the reduction step, the MHs were not uniformly coated on the rGO surfaces and were of poor crystallinity as shown in Fig. S1a, (ESI†). To obtain a uniform coating and

enhance crystallinity, the suspension obtained above was maintained at various hydrothermal synthesis temperatures of 90, 120, 150, and 180 °C for 10 h (Fig. S1b-e, ESI†).

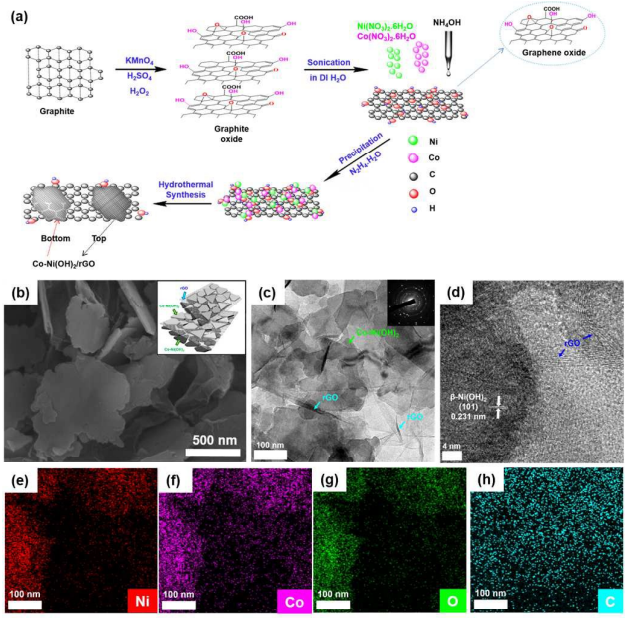

Fig. 1 (a) Schematic illustration of preparation processes of lamellar Co-Ni(OH)$_2$/rGO structures, (b) SEM image (inset shows the lamellar structure), (c) TEM image (inset shows the SAED pattern), (d) HRTEM, and (e-h) EDS mapping of Ni, Co, O, and C, respectively.

The lamellar Co-Ni(OH)$_2$/rGO structure is prepared at a GO to metal precursor ratio of 1:10 at 150 °C for 10 h. Fig. 1b and c respectively show FESEM and TEM images of lamellar Co-Ni(OH)$_2$/rGO structures prepared at the hydrothermal synthesis temperature of 150 °C. From the figures, it can be seen that binary MHs, Co-Ni(OH)$_2$, grew on the rGO surface and formed a uniform coat after hydrothermal synthesis. At RT (Fig. S1a, ESI†), the rGO surface was not fully covered with MHs, while plate-like structures consisting of both rGO and Co-Ni(OH)$_2$ were obtained after hydrothermal treatment. For the sample synthesized at RT, MH particles were deposited by co-precipitation on rGO sheets and were not able to diffuse well on rGO surface at low temperature, as was revealed by SEM. However, during hydrothermal synthesis the deposited particles were able to diffuse and recrystallize[9] into well-defined plate-like β-Ni(OH)$_2$ forms that uniformly coated the rGO surface and finally formed the lamellar structure. Coating can be at both the tops and bottoms of the rGO layers, as shown in Fig.1a-c. And rGO can also be sandwiched between the MH layers (Fig. 1c and Fig. S1c, ESI†). The crystallographic structure of Co-Ni(OH)$_2$/rGO composites was characterized by XRD (Fig. S1f, ESI†). It can be seen that all the peaks are well matched with peaks of α (003) (JCDPS No. 38-0715) and β ((001), (100), (101), (102), (110), and (111)) forms of Ni(OH)$_2$ (JCDPS No. 14-0117). The degree of crystallinity of the composites increased at elevated temperatures as their XRD patterns testify. A change in phase was also observed from the α form (for RT and 90 °C) to the β form (for temperatures > 90 °C) probably due to the removal of water and intercalated ions from the α form of Co-Ni(OH)$_2$ (Fig. S1f, ESI†). It is evident from the TEM image (Fig. 1c) that plate-like crystalline Co-Ni(OH)$_2$ coated the rGO sheets well. The corresponding SAED pattern (inset of Fig. 1c) confirms that the Co-Ni(OH)$_2$ arrays are polycrystalline structures. The HRTEM image in Fig. 1d reveals an interplanar spacing of 0.231 nm corresponding to the (101) plane of Co-Ni(OH)$_2$.[6] Furthermore, the EDS mapping of Ni, Co, O, and C shows uniform and continuous distribution over the entire rGO surface, which is a good sign of the formation of Co-Ni(OH)$_2$/rGO (Fig. 1e–h).

Further investigation to observe the effect of graphene oxide on the metal precursor ratio was performed at a fixed temperature of 150 °C. Among the samples the lamellar structures prepared at 150 °C gave higher Cs values and preeminent rate capabilities (Table S1, ESI†). Samples were synthesized with GO-to-metal precursor ratios of 1:10, 1:7.5, and 1:5 at 150 °C. At low and moderate amounts of GO, plate-like structures were obtained as shown in Fig. S2a and b (ESI†). However, as the amount of GO increased further, at the 1:5 ratio, the MHs tended to grow vertically (Fig. S2c, ESI†) on the rGO surface possibly because the growth time (10 h) was insufficient for the precipitated MHs to aggregate and form plate-like structures. The degree of crystallinity decreases with increasing amounts of GO and a high degree of crystallinity was observed at the 1:10 ratio (Fig. S2d, ESI†).

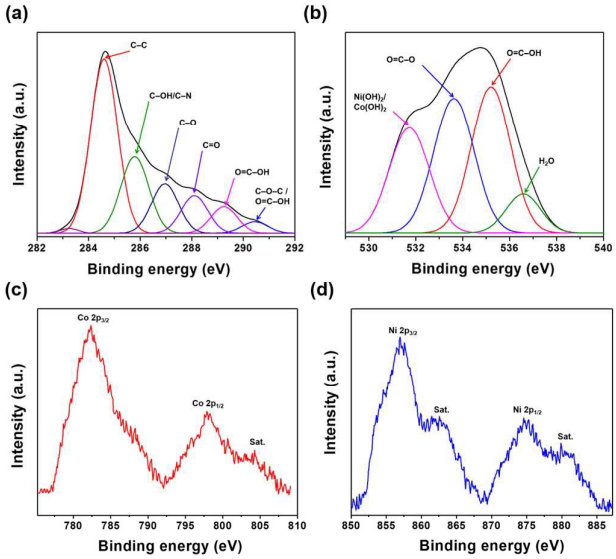

Fig. 2 (a) C 1s, (b) O 1s, (c) Co 2p, and (d) Ni 2p XPS spectra of lamellar Co-Ni(OH)$_2$/rGO prepared at 150 °C, 1:5 ratio, and 12 h.

XPS was applied to study the chemical states of the Co-Ni(OH)$_2$/rGO as prepared for 12 h. The complete survey spectrum is depicted in Fig. S5†. The main peaks observed were C 1s, O 1s, Co 2p, and Ni 2p. The narrow region of the spectrum of C 1s (Fig. 2a) was fitted by multiple peaks of C–C (284.6 eV), C–OH/C–N (285.8 eV), C–O (286.95 eV), C=O (288.1 eV), and O=C–OH (289.25 eV), and C–O–C/O=C–OH (290.45 eV).[24,25] The deconvoluted O 1s spectrum (Fig.

2b) demonstrates the formation of Co-Ni(OH)$_2$ at 531.7 eV[26,27] and the presence of the oxygen atoms of the relevant surface functional groups at 533.6 eV (O=C–O), 535.2 eV (O=C–OH), and 536.6 eV (adsorbed water and/or oxygen).[28-30] Co peaks were obtained at 782.36 eV and 797.8 eV, which are respectively ascribed to Co $2p_{3/2}$ and Co $2p_{1/2}$[26,31], implying the formation of Co-Ni(OH)$_2$/rGO (Fig. 2c). Two major Ni peaks with binding energies of 856.96 eV and 874.56 eV, with their corresponding satellite peaks, are attributed to Ni $2p_{3/2}$ and Ni $2p_{1/2}$, respectively (Fig. 2d). Their spin energy separation of 17.6 eV, which is in good agreement with previous reports, further verifies the formation of Co-Ni(OH)$_2$/rGO.[32,33]

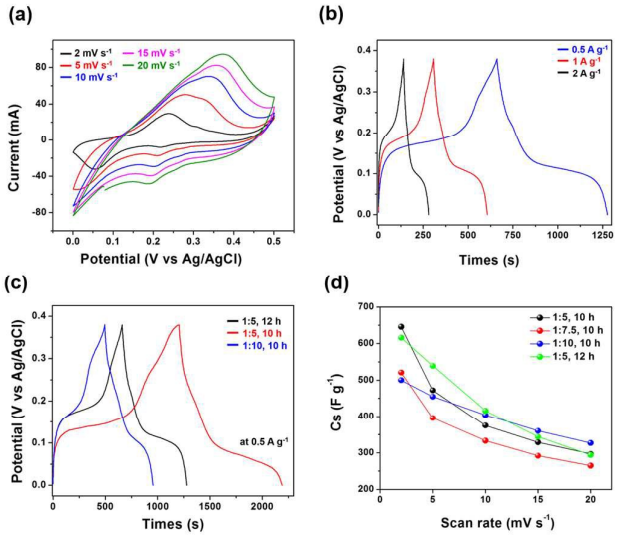

Fig. 3 (a) CV and (b) GCD curves of lamellar Co-Ni(OH)$_2$/rGO prepared at 150 °C, 1:5 ratio, and 12 h. (c) GCD curves of Co-Ni(OH)$_2$/rGO prepared at different GO to metal precursor ratios and synthesis times. (d) Comparison of Cs of lamellar Co-Ni(OH)$_2$/rGO prepared at different GO to metal precursor ratios and synthesis times.

The electrochemical property of the Co-Ni(OH)$_2$/rGO electrodes was studied using CV and GCD measurements (Fig. 3 and Fig. S4, ESI†). The figures suggest that the charge storage mechanism encompasses both pseudocapacitance and electric double-layer capacitance (EDLC), as is clearly shown from the peaks of the CV curves. The Faradaic pseudocapacitive characteristics may result from the binary redox couples of Co^{2+}/Co^{3+} and Ni^{2+}/Ni^{3+}.[18]

Cs values were calculated from the CV curves for different hydrothermal synthesis temperatures and for different scan rates and are given in Table S1 (ESI†). It is obvious that an increment in temperature resulted in higher Cs values. This can be due to the unique structure with its optimal coupling of MHs and rGO supporting facile ion diffusion and enhancing electronic conductivity at higher temperatures. Additionally, there is an increase in the degree of crystallinity with respect to temperature. At RT, the samples were of poor crystallinity. Low-crystallinity samples usually suffer from low electronic conductivity, which can be due to the presence of highly porous open microstructures. Thus, Cs values were increased with improved crystallinity. In addition, crystalline samples have good rate capability (Table S1, ESI†), which is due to the better electronic conductivity, which can also be explained from the EIS results (Fig. 4a). However, at 180 °C, the Cs value was relatively low because when materials become highly crystalline a simultaneous decrease in surface area occurs. Consequently, the protonation (or deprotonation) reaction will be limited, leading to lower Cs values.[34]

In addition to the effect of temperature on Cs values, the ratio of graphene oxide to metal precursor was scrutinized at 150 °C for 10 h. At the specified temperature, due to its unique porous structure which eases ion diffusion the sample prepared at a 1:5 ratio gave the highest Cs of 646 F g^{-1} at 2 mV s^{-1}, while the 1:7.5 and 1:10 ratios exhibited 521 F g^{-1} and 500 F g^{-1} at the same scan rate, respectively. However, it appears that their respective rate capabilities at 20 mV s^{-1} were dependent on their degree of crystallinity (1:5 ratio = 45.97 %) < (1:7.5 ratio = 50.86 %) < (1:10 ratio = 65.4 %) (Table S2a, ESI†). Moreover, the Cs values from GCD tests were calculated as 1294 F g^{-1}, 536 F g^{-1}, and 611 F g^{-1} for the samples prepared at 1:5, 1:7.5, and 1:10 ratios, respectively, at 0.5 A g^{-1}. Similarly, the rate capability based on the GCD tests of the crystalline samples, (1:10 ratio = 88.7 %) and (1:7.5 ratio = 86 %), dominated the sample of poor crystallinity (1:5 ratio = 68.86 %), at 2 A g^{-1} (Table S2b, ESI†). Although the Cs value 1294 F g^{-1} is too high for the low-crystallinity sample, its rate capability is very low. This might be because the crystalline samples possess good electronic conductivity but with compromised ionic transport, resulting in lower Cs values. On the other hand, the low-crystallinity sample could give a higher Cs at one end due to its porous open microstructures, but have poor rate capability on the other due to the lower electronic conductivity. Therefore, a trade-off is needed between the ionic transport (dominant for low-crystallinity samples) and electronic conductivity (higher for crystalline samples) of the electrodes. However, it is worth mentioning that of all the samples the Cs values are relatively higher when we consider that a higher mass loading, 4.5-5.5 mg cm^{-2}, was used compared to that of previous studies (Table S3, ESI†). Besides the unique structure and crystallinity of the lamellar structures, the other factor affecting the Cs values was considered to be the amount of GO used, which unquestionably can increase the Cs through its EDLC.

In order to maintain higher Cs with improved rate capabilities, our approach involved increasing the growth time of Co-Ni(OH)$_2$/rGO, which gave the highest Cs at 150 °C with growth times of from 10 to 12 h, and with a1:5 ratio - with the speculation that crystallinity can be enhanced with growth time and the crystalline sample can give rise to better rate capability. Co-Ni(OH)$_2$/rGO obtained at the same conditions, 150 °C and 1:5 ratio, but with an increased growth time of 12 h, was characterized using FESEM, TEM, HRTEM, and XRD. A similar lamellar Co-Ni(OH)$_2$/rGO structure was obtained, as revealed by the FESEM image (Fig. S3a, ESI†). It is evident from the TEM image that the coating of MHs on rGO is uniform (Fig. S3c, ESI†). Additionally, HRTEM (Fig. S3d ESI†) shows lattice spacings of 0.233 nm and 0.201 nm, respectively corresponding to the 101 (β form) and 004 (α form) atomic plane orientations of Co-Ni(OH)$_2$. From the XRD pattern (Fig. S3b, ESI†), it is obvious that increasing the growth time enhanced the degree of crystallinity, which confirmed our speculation.

CV and GCD tests were performed to further check whether or not the rate capability of the new lamellar crystalline sample, prepared at 150 °C with a 1:5 ratio and in 12 h, can be improved. As can be seen from Fig. 3a and 3b, redox peaks and symmetric charge discharge curves were observed to be the same as for the other samples. Cs values of 617 F g^{-1} at 2 mV s^{-1} and 811 F g^{-1} at 0.5 A g^{-1} were obtained. Fig. 3d also reveals that the new lamellar crystalline sample has better rate capability than the other samples when the scan rate was increased from 2 to 15 mV s^{-1}. A clear difference in rate capability was observed from the charge discharge test results, as shown in Table S2b (ESI†). It was found that samples prepared at 1:5, 1:7.5, and 1:10 ratios for 10 h respectively retained 68.86, 86, and 88.7 % of their initial Cs values, while the sample synthesized at a 1:5 ratio for 12 h remarkably demonstrated a 90 % capacitance retention when the current density was changed from 0.5 to 2 A g^{-1}. Surprisingly, the rate capability significantly increased from 68.86 to 90 % with the enhanced degree of crystallinity. Hence, the synergistic effect of high amounts of GO and crystallinity can give rise to both higher Cs and rate capability. This might be due to several reasons. First, the lamellar Co-Ni$(OH)_2$/rGO structure facilitates diffusion of electrolyte ions to access the electroactive sites on the composite. Second, rGO by itself is a good electrical conductor, so increasing its amount in the composite presumably increases electrical conductivity.[35,36] Third, a higher amount of rGO contributed to the EDLC in addition to serving as a conductive matrix to provide conductive networks for electron transport during the electrode reaction processes, which is favourable for stabilizing the electronic and ionic conductivities. Finally, and perhaps most importantly, as the samples become more crystalline, the electron transport in the electrodes was increased, demonstrating a higher rate capability than that of the samples of poor crystallinity.

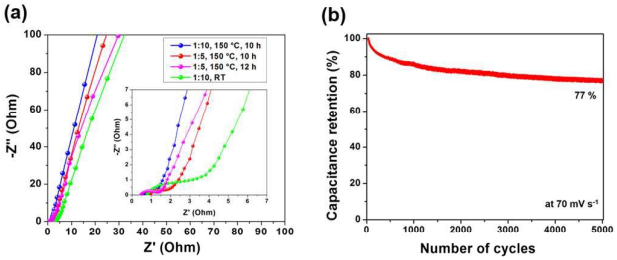

Fig. 4 (a) Nyquist plot of Co-Ni$(OH)_2$/rGO (RT ,150 °C and ratios of 1:10 and 1:5) and (b) Cycling stability of lamellar Co-Ni$(OH)_2$/rGO (at 150 °C,1:5 ratio, 12 h)

EIS measurements were performed to quantitatively evaluate electrical resistance, which is an important aspect of an SC electrode. Fig. 4a compares the Nyquist plot of Co-Ni$(OH)_2$/rGO, prepared at RT and at 150 °C at the ratios of 1:10 and 1:5 for 10 h and 12 h, measured with open circuit conditions in the frequency range of 1 mHz to 100 kHz. The plot consists of a semicircle at the high-frequency region, which is related to Faradic reactions (charge transfer), and a straight line at the low-frequency region. A nearly vertical straight line at low frequencies suggests that the kinetics of ion diffusion in the solution and the adsorption of ions onto the electrode surface occur swiftly. Bulk solution resistance, Rs, is related to electrolyte resistance, collector/electrode contact resistance, and electrode/electrolyte interface resistance.[37] The Rs values were ~0.48, ~0.625, ~0.933, and ~ 0.786 Ω for lamellar Co-Ni$(OH)_2$/rGO structures with(150 °C, 1:5 ratio, 12 h), (150 °C, 1:10 ratio, 10 h), (150 °C, 1:5 ratio, 10 h), and (RT, 1:10 ratio), respectively. The Co-Ni$(OH)_2$/rGO charge transfer resistance Rct was ~0.608 Ω with(150 °C, 1:10 ratio, 10 h), which is markedly less than the Rct values with(150 °C, 1:5 ratio, 12 h), (150 °C, 1:5 ratio, 10 h), and (RT, 1:10 ratio) that were respectively ~0.885 Ω, ~1.044 Ω and ~2.51 Ω. Smaller Rct values were obtained for the lamellar crystalline Co-Ni$(OH)_2$/rGO structures with (150 °C, 1:10 ratio, 10 h) and with (150 °C, 1:5 ratio, 12 h), suggesting that the combined effect of unique lamellar structures and a high degree of crystallinity greatly affect both ionic and electronic conductivity, hence affecting the Cs value. In addition, higher amounts of rGO in the composite (1:5 ratio) contributed to smaller resistance compared to the sample prepared at RT (1:10 ratio), since both samples were of low crystallinity. Finally, cycle stability, an important issue for capacitors for long-term applications, was examined. Fig. 4b shows the stability for the lamellar Co-Ni$(OH)_2$/rGO (150 °C, 1:5 ratio, 12 h), illustrating excellent stability and only a 23 % loss of Cs at 5000 cycles at a high scan rate of 70 mV s^{-1}. This capacitance retention is similar or better than that of previous studies.[4,38,39]

Conclusions

Lamellar structured crystalline Co-Ni$(OH)_2$/rGO was synthesized using co-precipitation followed by hydrothermal synthesis. The morphology results indicated the importance of the hydrothermal synthesis temperature, which significantly controlled the structure and degree of crystallinity of the Co-Ni$(OH)_2$/rGO. The electrochemical results demonstrated that crystalline samples have superior Cs values and retention compared to samples of low crystallinity. The amount of graphite oxide used was also the main factor that influenced the electrochemical performance, but it tended to decrease crystallinity when used in the higher amounts. To avoid this, the hydrothermal synthesis time was increased, from 10 h to 12 h, which allowed crystal growth and gave a crystalline sample. A higher value of Cs (617 F g^{-1} at 2 mV s^{-1} and 811 F g^{-1} at 0.5 A g^{-1}), the highest capacitance retention (~90 % at 2 A g^{-1}), and good cycle stability (~77 % at 70 mV s^{-1} at 5000 cycles) with lower resistance (Rs ~0.48 Ω and Rct ~0.885 Ω) were exhibited by the lamellar-structured Co-Ni$(OH)_2$/rGO prepared at 150 °C for 12 h at the ratio of 1:5. Improved Cs values and rate capabilities were obtained due to the unique lamellar structure and enhanced degree of crystallinity, which improved both ionic and electronic conductivity - as shown by the lower Rct value from the EIS results despite the fact that a higher mass loading approaching that of commercial supercapacitors was used.

Acknowledgements

This research was supported by Basic Science Research Program through the National Research Foundation of Korea

(NRF) funded by the Ministry of Education, Science and Technology (NRF-2013R1A2A2A01010027).

Notes and references

1 P. Simon and Y. Gogotsi, *Nat. Mater.*, 2008, **7**, 845.
2 J. R. Miller and A. F. Burke, *Electrochem. Soc. Interf.*, 2008, **17**, 53.
3 J. Chen, D. H. Bradhurst, S. X. Dou and H. K. Liu, *J. Electrochem. Soc.*, 1999, **146**, 3606.
4 Y. Cheng, H. Zhang, C. V. Varanasi and J. Liu, *Energy Environ. Sci.*, 2013, **6**, 3314.
5 A. Motori, F. Sandrolini and G. Davolio, *J. Power Sources*, 1994, **48**,361.
6 J. Chang, H. Xu, J. Sun and L. Gao, *J. Mater. Chem*., 2012, **22**, 11146.
7 X. H. Xia, J. P. Tu, Y. Q. Zhang, Y. J. Mai, X. L. Wang, C. D. Gu and X. B. Zhao, *J. Phys. Chem. C*, 2011, **115**, 22662.
8 P. Huang, C. Cao, Y. Sun, S. Yang, F. Wei and W.Song, *J. Mater. Chem.A*, 2015, **3**, 10858.
9 H. L. Wang, H. S. Casalongue, Y. Y. Liang and H. J. Dai, *J. Am. Chem. Soc.*, 2010, **132**, 7472.
10 Y. Gogotsi and P. Simon, *Science*, 2011, **334**, 917.
11 R. Liu, J. Duay and S.B. Lee, *Chem. Commun.*, 2011, **47**, 1384.
12 J. Maier, Nat. Mater., 2005, **4**, 805.
13 C.C. Hu, K.H. Chang, M.C. Lin and Y.T. Wu, *Nano Lett.*, 2006, **6**, 2690.
14 N.O. Weiss, H. Zhou, L. Liao, Y. Liu, S. Jiang, Y. Huang, and X. Duan, *Adv. Mater.*, 2012, **24**, 5776.
15 Y. Zhu, S. Murali, W. Cai, X. Li, J.W. Suk, J.R. Potts and R.S. Ruoff, *Adv. Mater.*,2010, **22**, 3906.
16 H. B. Liu, L. Xiang and Y. Jin, *Cryst. Growth Des.*, 2006, **6**, 283.
17 N. Mahmood, M. Tahir, A. Mahmood, W. Yang, X. Gu, C. Cao, Y. Zhang and Y. Hou, *Sci. China Mater.*, 2015, **58**, 114.
18 R.R. Salunkhe, K. Jang, S.W. Lee and H. Ahn, *RSC Adv.*, 2012, **2**, 3190.
19 X. Wang, W.S. Liu, X. Lu and P.S. Lee, *J. Mater. Chem.*, 2012, **22**, 23114.
20 W.S. Hummers Jr and R.E. Offeman, *J. Am. Chem. Soc.*, 1958, **80**, 1339.
21 D.R. Dreyer, S. Park, C.W.Bielawski and R. S. Ruoff,*Chem. Soc. Rev.*, 2010, **39**, 228.
22 S. Cabanas-Polo, K.S. Suslick, and A.J. Sanchez-Herencia, *Ultrason.Sonochem.*, 2011, **18**, 901.
23 C. Gómez-Navarro, R.T. Weitz, A.M. Bittner, M. Scolari, A. Mews, M. Burghard and K. Kern, *Nano Lett.*, 2007, **7**, 3499.
24 U. Zielke, K. J. Huttinger and W. P. Hoffman, *Carbon*, 1996, **34**, 983.
25 R.K. Birojuand P.K. Giri, J. Phys. Chem. C, 2014, **118**, 13833.
26 J. Yang, H. Liu, W.N. Martens and R.L. Frost, *J. Phys. Chem. C*, 2009, **114**, 111.
27 K.S. Kim and N. Winograd, *Surf. Sci.*, 1974, **43**, 625.
28 J.H. Zhou, Z.J. Sui, J. Zhu, P. Li, D. Chen, Y.C. Dai and W.K. Yuan, *Carbon*, 2007, **45**, 785.
29 L.Z. Fan, J.L. Liu, R. Ud-Din, X. Yan and X. Qu, *Carbon*, 2012, **50**, 3724.
30 D. Puthusseri, V. Aravindan, S. Madhavi and S. Ogale, *Energy Environ. Sci.*, 2014, **7**, 728.
31 U.M. Patil, M.S. Nam, J.S. Sohn, S.B. Kulkarni, R. Shin, S. Kang, S. Lee, J.H. Kim and S.C. Jun, *J. Mater. Chem.A*, 2014, **2**, 19075.
32 S. Oswald and W. Brückner, Surf. Interface Anal., 2004, **36**, 17.
33 H. Li, Y. Yu, M. Starr, Z. Li and X. Wang, *J. Phys. Chem. Lett.*, 2015, **6**, 3410.
34 Q. Yang, Z. Lu, J. Liu, X. Lei, Z. Chang, L. Luo and X. Sun, *Prog. Nat. Sci.*, 2013, **23**, 351.
35 S. Stankovich, D.A. Dikin, R.D. Piner, K.A. Kohlhaas, A. Kleinhammes, Y. Jia, Y. Wu, S. T. Nguyen and R.S. Ruoff, *Carbon*, 2007, **7**, 1558.
36 C. Liu, Z. Yu, D. Neff, A. Zhamuand B.Z. Jang, *Nano Lett.*, 2010, **10**, 4863.
37 Z. Wu, X.L. Huang, Z.L. Wang, J.J. Xu, H.G. Wang and X.B. Zhang, *Sci. Rep.*, 2014, **4**, 3699.
38 X. Chen, C. Long, C. Lin, T. Wei, J. Yan, L. Jiang and Z. Fan, *Electrochim. Acta*, 2014, **137**, 352.
39 H. Chen, L. Hu, M. Chen, Y. Yan and L. Wu, *Adv. Funct. Mater.*,2014, **24**, 934.

For TOC use only

Enhanced electrochemical performance of lamellar structured Co-Ni(OH)$_2$ /reduced Graphene Oxide (rGO) via hydrothermal synthesis

Sintayehu Nibret Tiruneh,[‡] Bong Kyun Kang,[‡] Quang Tran Ngoc and Dae Ho Yoon[*]

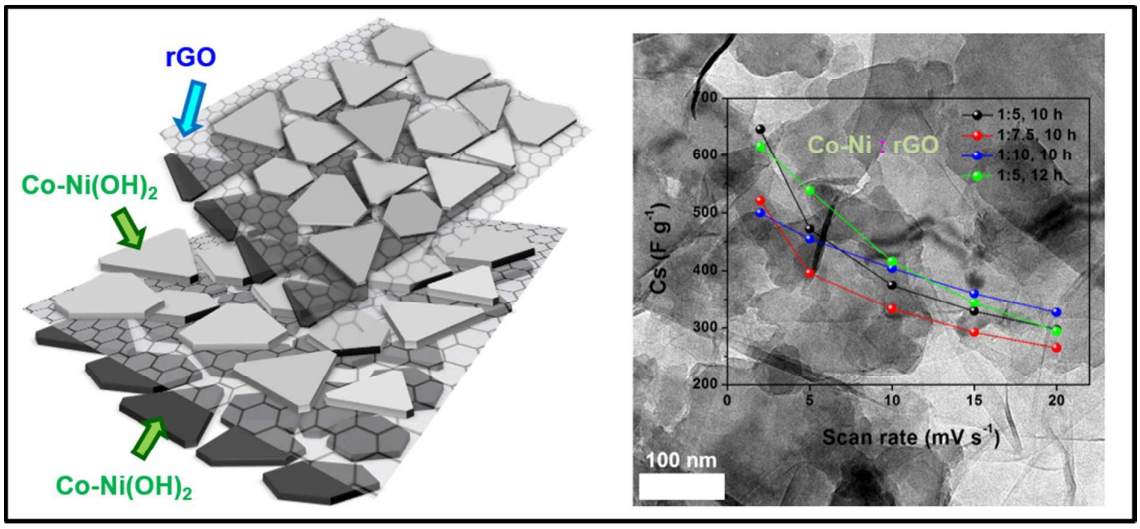

Lamellar Co-Ni(OH)$_2$/rGO structures were synthesized and their ionic and electronic conductivity were improved due to the unique structure and enhanced degree of crystallinity and exhibited long term stability even if high mass loading was used in electrode fabrication.